

Large eddy simulation of premixed flames in Couette flow

S. Menon

Georgia Inst. of Technology, Atlanta

V. K. Chakravarthy

Georgia Inst. of Technology, Atlanta

AIAA, ASME, SAE, and ASEE, Joint Propulsion Conference and Exhibit, 32nd, Lake Buena Vista, FL, July 1-3, 1996

Large eddy simulations in a wall bounded domain are conducted in order to study the kinematic structure of premixed turbulent flame. The linear model presents a prospect of isolating the effects of each of the physical mechanisms that underly turbulent combustion. In the present study, we investigate the flame structure in the absence of thermodynamic effects, such as heat release, using this model and compare the results to predictions arrived at using Yakhot's model. The momentum transport is modeled using an eddy viscosity approach based on the dynamic subgrid kinetic energy equation. The LEM approach is found to be fairly accurate in nonhomogeneous shear flows, such as the Couette flow. It is found that the effects of turbulence on the flame geometry are modeled well using this approach. The model, however, needs to be modified for the limiting case of near laminar propagation in regions of space with little or no turbulence. (Author)

Large eddy simulation of premixed flames in Couette flow*

S. Menon[†] & V. K. Chakravarthy[‡]
School of Aerospace Engineering
Georgia Institute of Technology
Atlanta, GA 30332-0150

Abstract

Large eddy simulations in a wall bounded domain are conducted in order to study the kinematic structure of premixed turbulent flame. The linear model presents a prospect of isolating the effects of each of the physical mechanisms that underly turbulent combustion. In the present study, we investigate the flame structure in the absence of thermodynamic effects such as heat release using this model and compare the results to predictions arrived at using Yakhot's model. The momentum transport is modeled using an eddy viscosity approach based on the dynamic sub-grid kinetic energy equation. The LEM approach is found to be fairly accurate in non-homogeneous shear flows such as the Couette flow. It is found that the effects of turbulence on the flame geometry are modeled well using this approach. The model however, needs to be modified for the limiting case of near laminar propagation in regions of space with little or no turbulence.

1 Introduction

The main goal of large eddy simulation (LES) is to simulate the large scale structure of the flow by accounting for the small scale effects using a model. Dissipation of kinetic energy is the only physical phenomenon of importance in non-reacting flows that occurs at small scales. Separating these small scales and the large scales (of the size of the characteristic geometric length in the flow) is the inertial range which acts purely as an energy cascade for supplying kinetic energy to the small scales from the large scales. The near universal behavior of the inertial range along with the assumption of local isotropy in this range have been used to model turbulent flows using the eddy viscosity assump-

tion. However, modeling of these small scale effects in scalar mixing/reactions is more complicated than in momentum transport, posing a bigger challenge in the field of continuum studies. There are various forms of scalar spectrum in the inertial and dissipative ranges depending on the local Schmidt number (or Prandtl number). Similar parameterization of scalar mixing using an eddy diffusivity, however, often seems to fail especially if the scalar is not passive. If the fluid is reacting, there are phenomena like the molecular mixing and chemical reactions occurring at smallest of the scales (Kolmogorov and Batchelor scales). These need to be adequately modeled within the constraints of available computational resources.

Computational approaches in mixing studies, in most cases, can be classified into two groups: moment methods and the probability density function (PDF) methods. In moment methods, the flow variables are decomposed into mean and fluctuating components. The numerical procedure involves solving for the mean values and a few lower moments (correlations) of chemical and fluid dynamic quantities. A comprehensive account on this method can be found in Ref[1] (Patterson, 1981). In the PDF approach, the objective is to arrive at the PDF of the chemical quantities. This approach is outlined in Ref[2] (Pope, 1985).

In moment methods, the reaction rate terms and the turbulent stirring term need to be modeled. Because of the nonlinearity of the reaction rate term, one needs a good global mechanism to cut down on the cost. Fast kinetics (infinite rate) further allow for reasonable approximations which seem to be valid for some hydrocarbon reactions. The turbulent fluxes are modeled using a gradient diffusion assumption. The turbulent diffusivity is obtained using passive scalar transport theories, which do not account for thermodynamic effects like heat release. Hence, the gradient diffusion assumption, while adequate for passive scalar transport, fails in case of reacting flows. Furthermore, in many practical engineering systems, combustion takes place in a regime of parameter space called the

[†] Associate Professor, Senior Member, AIAA.

[‡] Graduate Research Assistant.

* Copyright ©1996 by S. Menon & V. K. Chakravarthy. Published by the American Institute of Aeronautics and Astronautics, Inc., with permission.

corrugated flamelet zone. In this region of parameter space, the flame is wrinkled by turbulence but the local burning is laminar. The turbulent flame is an ensemble of local laminar flamelets whose size spans over several decades of length scales. Hence, there are reaction zones that occur with characteristic length scales extending to such small values that molecular diffusion becomes very significant. The molecular diffusion is what causes the local laminar propagation. However, in the moment methods, the effects of molecular diffusion cannot be captured adequately. Further, the moments chosen that are used to characterize the chemistry in a flow field are arbitrary. It cannot be based on numerical values of these moments because some moments, while insignificant in terms of quantities, need to be predicted accurately (eg. NO_x emissions).

In PDF methods, the solution is arrived at, in either of the two ways: evolve a PDF in time using a dynamic equation or assume a specific form for the PDF in terms of a few parameters and predict their values by modeling. The assumed PDF method was extended for LES by Frankel et al. (1993). Gao and O'Brien (1993) suggest solving the PDF evolution equation (Pope 1990) for LES. Their work is far from complete and needs further development. The PDF methods have one main advantage that the chemical reaction term is closed. Molecular diffusion needs to be modeled and is usually done using variants of the coalescence-dispersion models. This aspect is the subject of ongoing research and at the present day greatly limits the capability of the PDF models.

When the reaction system is dominated by one physical phenomenon, there are several models that work well. Yakhot's model[6], Fractal models[7](for premixed combustion with low or no heat release) that concentrate on the kinematic structure of the flame and characterize the model in terms of incoming turbulence, Fureby and Moller model[8] which uses the turbulent reaction rate based on local turbulent and chemical time scales, are a few examples. Such models are far from representing the correct physics in many cases and are approaches suitable for case based model development studies.

A field equation for interface propagation [9] called the G -equation is used in this scalar transport study. This model was used earlier by several researchers to study the structure of a self propagating front in unsteady flow fields [9]. When the self-propagation speed is set equal to the laminar flame speed, any level surface of this scalar in space could be considered a cold flame. The primary advantage of the G -equation approach is the explicit inclusion of the flame

speed in the equation, thereby avoiding the need for solving the finite rate kinetics in multiple scalar equation.

Using the G -equation as representative of all the chemistry, the kinematic structure of premixed flames in a wall bounded shear flow is investigated. A linear eddy model [18] is used to model the subgrid combustion related processes and a subgrid kinetic energy equation model with dynamic evaluation of the model coefficients is used as the subgrid model for momentum transport. A turbulent Couette flow is chosen for the present study, because it has a wide core region with near constant values of *rms* velocity fluctuations. The turbulent intensity is then nearly constant in this region and when the flames are contained in here, the near constant value of the turbulence intensity can be used as a reference value for characterization of the results. All level G -surfaces enclosed fully in this region are considered to be flames and this gives several realizations of the flame to collect statistics over. The linear eddy model(LEM) is capable of accounting for the thermodynamic effects such as volumetric dilatation, viscosity variation with temperature etc. Heat release and finite rate chemical kinetics can be accounted for in this subgrid model in a deterministic way which makes stochastic part of the algorithm more crucial. So, we choose to investigate the LEM predictions of the kinematic structure of the flame using cold chemistry model. The results are compared to predictions from conventional LES using the Yakhot's model (which is known to predict reasonably correct values of the turbulent flame speed for $\frac{u'}{S_l}$ between 1 and 10). Here, u' is the turbulent intensity and S_l is the laminar flame speed.

An outline of the numerical and the LES model method are provided in section 2 and section 3 respectively. The linear eddy model is formulated in section 4. In section 5 are discussed the results from this study and the possible directions for future research are proposed.

2 Numerical method

The Navier-Stokes equations, on convolution with a spatial filter, reduce to the following set of LES equations.

$$\frac{\partial \bar{U}_i}{\partial x_i} = 0 \quad (1)$$

$$\frac{d\bar{U}_i}{dt} = -\frac{\partial \bar{p}}{\partial x_i} + \nu \frac{\partial^2 \bar{U}_i}{\partial x_k \partial x_k} + \frac{\partial \tau_{ij}}{\partial x_j} \quad (2)$$

where the overbar indicates a filtered variable, $\tau_{ij} = (\bar{U}_i \bar{U}_j - \bar{U}_i \bar{U}_j)$ is the subgrid stress. For a closed set of

equations, one needs to approximate the subgrid stresses using a model. The velocity variations in the scales below the characteristic filter width Δ are unresolved in a LES. Due to the nonlinear nature of the Navier-Stokes equations, these small scale fluctuations effect the large scale motions. This effect comes from the subgrid stress, which in the present study is approximated as $\tau_{ij} = -\frac{2}{3}K\delta_{ij} + 2\nu_t\overline{S_{ij}}$, where $\overline{S_{ij}} = \frac{1}{2}\left[\frac{\partial\overline{U_i}}{\partial x_j} + \frac{\partial\overline{U_j}}{\partial x_i}\right]$ is the resolved strain tensor, ν_t is subgrid eddy viscosity (to be defined later) and $K = -\frac{1}{2}(\overline{U_i U_i} - \overline{U_i}\overline{U_i})$ is the subgrid kinetic energy. Filtered variables are also called supergrid variables because they carry information about a variables at all length scales above the filter width (grid spacing). The model equations for the subgrid kinetic energy and the eddy viscosity are presented in the next section. The equations are discretized on a non-staggered grid (with spacing corresponding to the characteristic filter width Δ) and numerically integrated using a two step semi-implicit fractional step method. In this method, all of the primitive variables are defined at the grid points. The well known checker board type oscillations occur in velocity field due velocity-pressure decoupling when one uses central finite difference schemes for approximating the spatial derivatives. Use of QUICK scheme for calculation of velocity gradients that arise in the source term of the elliptic equation for pressure is found to effectively couple the velocity and pressure fields thus removing these oscillations [10]. The convective terms are computed using a third-order upwind biased finite difference approximation while the viscous terms are computed using a fourth-order central difference approximation. The Poisson equation is solved numerically using a second order accurate elliptic solver that uses a four-level multigrid scheme to converge the solution. The finite difference equations are integrated in time using a second order scheme.

The G -equation discussed earlier, has the following form.

$$\frac{\partial G}{\partial t} + u_j \frac{\partial G}{\partial x_j} = S_l |\nabla G| \quad (3)$$

and G lies between two constant values. When using Yakhot's model for LES, the advection velocity in the above equation if replaced by filtered velocity and the laminar flame speed by the turbulent flame speed. The Renormalization Group theory [Yakhot,1988] provides the following expression for the turbulent flame speed u_t .

$$\frac{u_t}{S_l} = \exp\left[\frac{u'^2}{u_t^2}\right] \quad (4)$$

where u' here, is the *rms* of (incoming) subgrid velocity

field (can be estimated using the subgrid kinetic energy). The numerical scheme used to calculate the gradient in the propagation term of eq.(3) is biased in the direction of maximum gradient.

3 LES Model

A K -equation model with dynamic evaluation of the model coefficients based on the Germano's filtering approach [11], is used as the subgrid model. The advantage of this model is that it solves a single scalar equation for the subgrid kinetic energy which characterizes the velocity scale of subgrid turbulence. This velocity scale along with the length scale (grid spacing or the filter width) provides a subgrid timescale representing the non-equilibrium relaxation of the subgrid scales. This is one level higher (in the direction of developing non-equilibrium models) than the equilibrium models (algebraic or the zero equation models), wherein the production and dissipation of the subgrid kinetic energy are assumed to balance instantaneously.

Menon and Kim [11] recently suggested a dynamic modeling approach using the K -equation. Only an outline of the model is provided here, since a more comprehensive description, including the implementation issues, can be found in Ref.11. The eddy viscosity and subgrid dissipation in physical space, for a characteristic filter width Δ , are given as follows.

$$\nu_t = C_\nu K^{\frac{1}{2}} \Delta, \quad (5)$$

$$\epsilon^{sgs} = C_\epsilon \frac{K^{\frac{3}{2}}}{\Delta} \quad (6)$$

For the transport term, a gradient diffusion model based on eddy diffusivity model (with unit eddy Prandtl number) has been proposed and studied by Menon and Kim. This approximation was found to adequately model the transport terms. Hence this is used in a similar form in this study. The dynamic equation for K can now be written as:

$$\frac{\partial K}{\partial t} + \overline{U_j} \frac{\partial K}{\partial x_j} = \tau_{ij} \frac{\partial \overline{U_i}}{\partial x_j} - \epsilon^{sgs} + \frac{\partial}{\partial x_j} \left[\nu_t \frac{\partial K}{\partial x_j} \right] \quad (7)$$

C_ν and C_ϵ are the model constants that need to be specified. These constants, however, are not universal and differ with flow fields in general. This suggests that these constants also depend on the local (supergrid) structure of the flow field. It is, then appropriate to refer to them as coefficients rather than constants. A dynamic approach is applied

here to evaluate these coefficients, thus removing the arbitrariness in prescribing these coefficients. The approach is based on the concept of subgrid stress similarity supported by experiments in jets (Liu et al. [12]). In this approach, a test filter (similar to the LES filter) of characteristic width 2Δ is defined and the corresponding filtered velocity field is denoted by \widetilde{U}_i . This new velocity field is obtained by convolution of the LES filtered velocity with the test filter. The subgrid stress corresponding to the scales in between the grid filter width and the test filter width can be written as [11]:

$$t_{ij} = \widetilde{U}_i \widetilde{U}_j - \widetilde{U}_i \widetilde{U}_j \quad (8)$$

and the corresponding dissipation is defined as

$$e = (\nu + \nu_t) \left[\frac{\partial \widetilde{U}_i}{\partial x_j} \frac{\partial \widetilde{U}_i}{\partial x_j} - \frac{\partial \widetilde{U}_i}{\partial x_j} \frac{\partial \widetilde{U}_i}{\partial x_j} \right] \quad (9)$$

Assuming stress similarity and the present model to be valid for length scales between Δ and 2Δ (which imposes a further restriction that the test filter width is also in the inertial range of length scales), t_{ij} and e can be written as follows.

$$t_{ij} = -\frac{2}{3} \widetilde{K} \delta_{ij} + 2\widetilde{\nu}_t \widetilde{S}_{ij} \quad (10)$$

and

$$e = C_\epsilon \frac{\widetilde{K}^{\frac{3}{2}}}{2\Delta}, \quad (11)$$

where $\widetilde{K} = -\frac{1}{2} t_{ii}$ and $\widetilde{\nu}_t$ is the eddy viscosity corresponding to the test filter of width 2Δ and is given by $C_\nu \widetilde{K}^{\frac{1}{2}} (2\Delta)$. From eq.(11), the value of C_ϵ can be evaluated. There are, however, six equations represented by eq.(10) using which C_ν could be evaluated. This is a over-determined system of equations and in the present formulation, is solved using least-squares technique. These coefficients are then used for evaluation of eddy viscosity and to advance the dynamic equation for K in time, thus achieving complete closure.

Now, the turbulent flame speed needed for subgrid closure of G -equation is computed using eq.(4). The value of u' needed in this equation is computed using the subgrid kinetic energy.

4 Linear Eddy subgrid model

A subgrid model should be able to account for all the relevant physical phenomena and couple well with the supergrid simulation. It should further allow for simulation of

real life physical problems efficiently within the constraints of available computational resources.

A subgrid model based on Linear eddy mixing model (Kerstein, 13-16) was proposed by Menon et al. (17-19). This model treats separately the two basic physical processes that govern the evolution of a reactive system: molecular diffusion (accounted for in the present formulation by prescribing the laminar flame speed) and turbulent stirring. The physics involved in the modeling procedure is outlined here and the mathematical detail is avoided.

The modeling is done on a representative one-dimensional spatially linear domain (contained in each LES cell). The effect of three dimensional eddies is accounted for, on this one dimensional domain using turbulent scaling laws [19]. This reduced representation was found to be fairly accurate for the purpose and leads to a substantial reduction in computational cost. The physical sense of the one dimensional domain depends on the investigation at hand. For example, it is a radial line while investigating the radial dispersion in circular jets, it is an axial line in studies involving axial transport. In homogeneous turbulence, it is a space curve aligned with the local scalar gradient. In LES, it is an arbitrary curve contained within each finite volume cell.

On the one-dimensional domain, the propagation and stirring are carried out as follows. Propagation is implemented by numerical simulation of G -equation without the convective term, using a finite volume approach on the linear domain. The G -equation now has the following one dimensional form.

$$\frac{\partial G}{\partial t} = S_l |\nabla G| \quad (12)$$

This equation replaces the one dimensional diffusion-reaction equation in the original formulation (for the finite rate kinetics). $G = 0$ corresponds to an unburnt state and $G = 1$ corresponds to a fully burnt state. Any surface in between can be considered to be the flame. The subgrid domain has no particular orientation (no directional information is included) and hence, periodic boundary conditions can be prescribed at the boundaries. The length of the domain is fixed to be the characteristic filter width used in the LES. The way to prescribe the number of cells needed for a finite volume implementation of the above equation is explained later. So the linear domain is a periodic curve of length Δ with arbitrary orientation and is fully contained in the LES cell. The convective term is dropped as the effect of subgrid fluid turbulence (stirring) is modeled separately.

More details are given elsewhere (Menon et al. 1993).

The turbulent stirring is modeled by a stochastic process. The sense of subgrid field is, hence, statistical. It is one realization of the field. A Lagrangian rearrangement is chosen as a means to model the effect of fluid dynamic eddies on the scalar gradient. The size of the eddy (needed to determine the size of the segment in which rearrangement is to be done) and the frequency of occurrence is determined using scaling laws characteristic of the inertial range. The rearrangement mapping can be chosen arbitrarily. It should mimic the effect of an eddy on scalar rearrangement in turbulence and also should be conservative (total species concentration should remain unaltered after the mapping). A triplet map [16] is chosen for the present study. In this mapping, the given segment of the linear domain is divided into three equal parts. The spatial gradients (of all properties) in the left and the right segments are increased by a factor of three. The middle segment is reversed and then the scalar gradients are scaled by a factor of three. As illustrated in the fig.1, the scalar field remains continuous and the mapping is conservative. Size of the subgrid finite volume cell is so chosen that a stirring event at the smallest relevant length scale could be executed using this mapping. In the present case, the smallest significant length scale is the Kolmogorov length scale and one needs at least six points to be contained in this length to perform stirring. So the number of cells turn out to be $6\frac{\Delta}{\eta}$. This mapping causes a particle dispersion with mean square displacement of $\frac{4}{27}l^2$, where l is the length of the segment. The diffusivity associated with this process can be determined to be $\frac{2}{27}\lambda l^3$, where λ is the frequency per unit length. The diffusivity associated with the eddies of length scale l is given by inertial range scaling laws as:

$$D_t = \left[\frac{l}{\eta} \right]^{\frac{4}{3}} \quad (13)$$

where η is the Kolmogorov length scale. Let $f(l)$ be the probability density function of the length scale chosen for the mapping event. By equating the diffusivity associated with the length scale l to the expression in the previous equation, the form of the PDF can be arrived at as:

$$f(l) = \frac{5}{3} \frac{l^{-\frac{4}{3}}}{\eta^{-\frac{4}{3}} - L^{-\frac{4}{3}}} \quad (14)$$

where L is the largest scale for stirring. In the present context of LES, it would equal Δ (all the eddies larger than Δ stir the scalar field at the supergrid level). Solving for λ yields

$$\lambda = \frac{54}{5} \frac{\nu Re_L}{L^3} \frac{\left[\frac{L}{\eta} \right]^{\frac{4}{3}} - 1}{1 - \left[\frac{\eta}{L} \right]^{\frac{4}{3}}} \quad (15)$$

where $Re_L = \frac{Lu'}{\nu}$ (the subgrid Reynolds number in the present case).

Heat release causes density gradients in the subgrid linear domain. When the density changes in a finite volume cell, the size of the cell is increased to conserve the mass in each cell. The domain is regrided to a uniform domain for computational ease. In the present case, there is no heat release or density variation, so this procedure is not required. For details on issues regarding heat release, see Smith and Menon[20].

Advection due to the supergrid velocity field brings about transport of the chemical species into the neighbouring LES cells. This is modeled using a procedure called "splicing" (Menon et al., 1993). The scalar flux across each LES cell face is computed using the supergrid velocity field. The number of cells that need to be transferred from one cell (donor cell) to its neighbouring cell (receiver cell) across this face is computed using this flux and the LES timestep. A segment with this number of cells is picked at random from the donor cell and inserted at a randomly chosen location on the linear domain in the receiver LES cell. This introduces discontinuities in the scalar concentration in the subgrid field. While this seems unphysical, splicing is a rare event compared to the subgrid processes and any spurious effects of splicing on the subgrid field is minimal. For further details on the implementation, see McMurtry et al. [21].

For each value of $\frac{u'}{S_1}$, simulations are conducted using various different realizations of a statistically stationary flow field as initial conditions. The flame is activated in a similar way in all the simulations. This is done by instantaneously changing the value of G from 0 to 1 in a cubical domain at the centre of the domain.

5 Results and discussion

LES of turbulent Couette flow at $Re = 5200$ (chosen due to availability of accurate data in literature) was conducted on two different grid resolutions. A streamwise length of πH and span-wise length of $\frac{1}{2}\pi H$, where H is the width of the channel, are used in these simulations. No slip boundary conditions are used in the wall normal direction and periodic boundary conditions are used in the other two directions. A $49 \times 33 \times 33$ grid reproduces *rms* of fluctuating

velocities favorably with DNS due to Bech et al. [22]. The grid is clustered near the walls and a y^+ of 0.3 is used as minimum wall normal resolution. These single point statistics are shown in fig.2. There is significant amount of kinetic energy in the subgrid scales at this resolution, so *rms* values of fluctuating velocities should be underpredicted. As can be seen, *urms* is overpredicted by the LES. This is a well noted [23] fact that is true when the axial resolution is inadequate. This overprediction is not expected to alter greatly the flame evolution. The results corresponding to the 25x17x17 LES are presented in fig.3. The trends in prediction, in terms of single point statistics, are as expected. The predictions differ significantly, possibly due to a broad range of energetic scales (subgrid kinetic energy is found to be quite significant). The cutoff scale in these simulations borders on dissipation range of scales. Hence, for the sake of implementing LEM (which requires the cut off scale in the inertial range), a higher Re (=12000) is chosen. The LES resolution is increased accordingly to 65x49x49. The 25x17x17 grid is however retained. The subgrid kinetic energy predictions by LES on these grid resolution are shown in fig.4. The finer grid resolves the shear layer and captures the kinetic energy peak near the wall. The coarse grid does not have adequate resolution near the wall. A y^+ of 4.0 was used for wall normal resolution near the wall. The simulation retains stability but the near wall results are not expected to be correct. Since the focus here, is on the core region, this fact is not of much concern.

The variation of the model coefficients with the wall normal coordinate in this simulation is shown in fig.5. While the values are of the same order of magnitude as in constant coefficient K -equation models, they are found to be lower by a few times. The C_ϵ values are close to it's suggested value of 0.916, but C_ν values are about three times lower than recommended constant value of 0.0854.

While implementing LEM in LES, the laminar flame speed is fixed by prescribing $\frac{u'}{S_L}$, where u' is based on core region turbulent intensity (which is nearly a constant over a wide region).

For the 65x49x49 grid, the volume occupied by the burnt gases (volume integral of G over the whole domain) is plotted against time for three different values of $\frac{u'}{S_L}$: 1, 4 and 8, in fig.6. The corresponding predictions from LES using Yakhot's model are also presented for comparison. This gives the quantitative measure of the flame growth. The comparison is favorable for $\frac{u'}{S_L}$ of 4 and 8, but the flame growth seems to be faster in case of Yakhot's model for $\frac{u'}{S_L}$ of 1. This perhaps could be attributed to the incorrect

flame propagation across the supergrid cells brought about by splicing. Splicing is a stochastic algorithm which works in the statistical sense (when averaged over several realizations). Further, the splicing should retain the same number of linear eddy cells in each of the LES cells since the fluid is incompressible. However, it is found that this is not the case. The number of cells in each LES cell is found to change by two cells in the worst case. The number of subgrid cells used in each LES cell is 50, which corresponds to the maximum subgrid Reynolds number (18.0) encountered in this LES. This is a conservation error that needs to be corrected in the future.

As mentioned earlier, each G -surface is considered a flame. Here iso-surfaces of G between 0.1 and 0.9 have been used as flames to collect flame statistics. The analysis of all geometric properties is considered next at a non-dimensional time of 0.4 (non-dimensionalized using channel width and laminar flame speed). Since the flow field is not stationary, several realizations corresponding to large eddy simulations with different initial fluid dynamic states (realizations of a statistically stationary fluid dynamic state) are used in calculation of these statistics.

A measure for characterizing the flame shape called the shape factor is defined as the ratio of smaller to higher eigen-values of the curvature tensor (Ashurst, 1993). It is bounded between -1 and 1. These extreme values correspond to a saddle and a spherical nature of the flame at a point, respectively. The value of 0 indicates a cylindrical structure. This value is computed at several points and a PDF is plotted for the three values of $\frac{u'}{S_L}$ in fig.7, fig.8 and fig.9. The figures indicate a cylindrical propagation of the flame, which is expected due to the shearing effect of Couette flow. There however, seem to be more locations on the flame predicted by LEM with locally spherical or saddle-type structure. This indicates more flame wrinkling by LEM. The Yakhot's model however is implemented using a supergrid field equation and wrinkling is based on the front propagation algorithm. It is difficult to distinguish between flame wrinkling due to turbulence and the spurious oscillations that are a characteristic of numerical methods used to capture scalar fronts using field equations. A DNS using G -equation with a more accurate numerical method for capturing scalar fronts would perhaps give the correct nature of the flame.

The mean curvature PDF is plotted for the three $\frac{u'}{S_L}$ values in fig.10, fig.11. and fig.12. This gives us a measure of local curvature of the flame. Predominant positive curvature indicates a convex flame growing outwards. In the

present study the PDF has a peak in the positive region. There however, are several points where the mean curvature is negative indicating that the flame shape is locally concave (and hence that the flame is wrinkled). Except for the lower value of $\frac{u'}{S_l}$, the results compare favorably to the Yakhot's model predictions.

The data from LES is now used to estimate the flame stretch (in the plane of the flame) which is defined as the rate of change of a Lagrangian flame surface element. It can be expressed in terms of local tangential strain rate, flame curvature and flame speed as (Candel and Poinso, 1990):

$$\kappa = -n_i e_{ij} n_j - \frac{S_l}{R} \quad (16)$$

where κ is the stretch, e_{ij} is the resolved scale strain tensor, in the plane of the flame and R is the mean principle radius of curvature. Positive stretch tends to decrease the flame speed and replanarize the flame, while negative stretch wrinkles the flame and increases propagation rate. The PDFs for flame stretch for the three $\frac{u'}{S_l}$ values are shown in fig.13, fig.14 and fig.15. As in the case of curvature, the results for the lower value of $\frac{u'}{S_l}$ do not compare well with Yakhot's model.

In case of $\frac{u'}{S_l}$ equal to 1.0, the laminar flame speed is a dominant factor in flame propagation. Turbulence effects are less significant in this case. The capability of a model such as LEM for predicting the correct propagation would depend greatly on the advection (splicing) algorithm. Since the present algorithm is stochastic, it perhaps is not suited for prediction of a near laminar (deterministic) propagation of the flame. An improvement to correct this inadequacy would be the objective of the future research, before the thermodynamics effects such as heat release are included.

The results from 25x17x17 grid are plotted against LES results obtained using Yakhot's on a 65x49x49 grid. It is very unlikely that the 25x17x17 grid would resolve the fine grain turbulent structure of the flame, but the large scale characteristics like the growth in size of the flame could turn out to be reasonably accurate. However, since the grid is coarse, if there exists an inertial range in Couette flow at $Re = 12000$, it is likely that the grid spacing would lie in the inertial range. Furthermore the subgrid Reynolds number in the core region is found to be of the order of 100 as against 20 in the 65x49x49 LES. The LEM was designed as a high Reynolds number model, so it is better to have a high subgrid Reynolds number. The volume occupied by burnt gases versus the time is plotted in fig.16. The pdfs for the ratio of curvatures and flame stretch are plotted in fig.17

and fig.18 respectively. In all these plots, the corresponding results from 65x49x49 LES using Yakhot's model are presented for comparison. It is seen that net growth of the flame is predicted fairly well. Also the pdf for the ratio of curvatures compares favorably with results from Yakhot's model. It is surprising that this prediction is more accurate than in the high resolution simulation. A higher Reynolds number in the subgrid could be one of the reasons for this. The statistics from the low resolution are not expected to be very accurate since they are based on numerical derivatives which can only account for the large scale structures and not the wrinkling at small scales. As can be seen in fig.18, the pdf of flame stretch is not as accurate as in the case of higher resolution case. The accurate prediction of mean curvature pdf could purely be heuristic.

6 Conclusions

The Linear eddy model is found to capture all the trends in the evolution of the flame structure. For the two higher cases of $\frac{u'}{S_l}$, the results are found to be close predictions obtained using Yakhot's model. The only issue of concern seems to be the difference in the prediction of the shape factor. This obviously is due to difference between the two methods in accounting for the advection due to supergrid velocity. In LES using Yakhot's model, the correct evolution of the sharp flame front is not captured in the early stages (due to reasons stated earlier). And in case of LEM, there is some randomness involved in the approach. There is no reason to believe one is more correct than the other. But the random nature of splicing is also the reason why the prediction of the flame structure in the case of near laminar (deterministic) propagation ($\frac{u'}{S_l}=1$) is found to be different. The splicing procedure may need to be modified in such cases.

The accurate prediction of flame growth in 25x17x17 is, however, very encouraging, a fact that warrants further research on LEM implementation in LES on grids coarse enough to be computationally efficient.

Acknowledgements

This research was supported by the NASA Lewis Research Center under Grant No. NAG3-1610 and by the Office of Naval Research under Grant N00014-93-1-0342. The authors acknowledge the help rendered by T. M. Smith, graduate student at the Georgia Institute of Technology, during the course of this research. The computer time was pro-

the HPC Center, Army Research Laboratories, Maryland.

References

1. Patterson, G. K., Application of turbulence fundamentals to reactor modeling and scaleup. *Chem. Eng. Commun.* 1981, 8, 25.
2. Pope, S. B., PDF methods for turbulent reactive flows. *Prog. Energy Combust. Sci.* 1985, 11, 119.
3. Frankel, S. H., Adumitroaie, V., Madnia, C. K. and Givi, P. Large eddy simulation of turbulent reacting flows by assumed PDF methods. *Engineering Application of Large Eddy Simulations*. 1993, ASME-FED-Vol.162, 81-101.
4. Gao, F., and O'Brien, E. E. A large eddy simulation scheme for turbulent reacting flows. *Phys. Fluids A*, 1993, 5, 1282-1284.
5. Pope, S. B. PDF methods for turbulent combustion: Progress and challenges, *Twenty third symposium (Int.) on combustion*, 1990, The Combustion Institute, 591-612.
6. Yakhot, V. Propagation velocity of premixed turbulent flames. *Combust. Sci. Tech.* 1988, 60, 443-450.
7. Menon, S. and Kerstein, A. R. Stochastic simulation of the structure and propagation rate of turbulent premixed flames. *Twenty fourth symposium (Int.) on combustion*, 1992, The Combustion Institute, 443-450.
8. Fureby, C. and Moller, S.-I. Large eddy simulation of reacting flows applied to bluff body stabilized flames. *AIAA J.*, 1995, 12, 2339-2347.
9. Kerstein, A. R., Ashurst, W. and Williams, F. A. Field equation for interface propagation in an unsteady homogeneous flow field. *Physical Review*, 1988 A37, 2728-2731.
10. Yan Zang, R. L. Street, and J. R. Koseff. A non-staggered grid, fractional step method for the time-dependent incompressible Navier-Stokes equations in curvilinear coordinates, *J. Comp. Phys.*, 1994, 114, 18-33.
11. Menon, S., and W.-W. Kim. High Reynolds number flow simulations using the localized dynamic subgrid scale model, *AIAA Paper 96-0425*, 34th Aerospace Sciences Meeting and Exhibit, Reno, NV.
12. Liu, S., Meneveau, S. and J. Katz, On the properties of similarity subgrid scale models as deduced from measurements in a turbulent jet," *J. Fluid Mech.*, 1994 275, 83.
13. Kerstein, A. R. Linear eddy model of turbulent scalar transport and mixing. *Combust. Sci. Tech.*, 1988, 60, 391-421.
14. Kerstein, A. R. Linear eddy model of turbulent transport II. Application to shear layer mixing. *Comb. Flame*, 1989, 75, 397-413.
15. Kerstein, A. R. Linear eddy model of turbulent transport III. Mixing and differential molecular diffusion in round jets. *J. Fluid. Mech.*, 1990, 216, 411-435.
16. Kerstein, A. R. Linear eddy model of turbulent transport. Part 6: Microstructure of diffusive scalar fields. *J. Fluid. Mech.*, 231, 361-394.
17. Menon, S. A new subgrid model for large eddy simulations of turbulent reacting flows, *QUEST Technical Report No. 595*, NASA Contract No. NAS2-13354, 1991.
18. Menon, S., McMurtry, P. A., and Kerstein, A. R. A linear eddy subgrid model for turbulent combustion: Application to premixed combustion, *AIAA paper 93-0107*, *AIAA 31st Aerospace Sciences Meeting*, Reno.
19. Menon, S., McMurtry, P. A. and Kerstein, A. R. A linear eddy mixing model for LES of turbulent combustion, in *LES of Complex Engineering and Geophysical flows* (Galerpin, B. and Orszag, S. ed.), Cambridge Univ. Press (1994).
20. Smith, T., and Menon, S. Model Simulations of freely propagating turbulent premixed flames. Paper No. 26-290, to be presented at the *Twenty sixth symposium (Int.) on combustion*, July 28 - August 2, 1996, Naples, Italy.
21. McMurtry, P. A., Menon, S., and Kerstein, A. R. A subgrid mixing model for LES of non-premixed turbulent combustion, *AIAA paper 92-0234*, *AIAA 30th Aerospace Sciences Meeting*, Reno.
22. Bech, K. H., Tillmark, N., Alfredson, P. H., and Anderson, H. I. An investigation of turbulent plane Couette flow at low Reynolds numbers, *Combust. Sci. Tech.*, 1995, 286, 291-327.
23. Askelvoll, K. and Moin, P. Large eddy simulation of turbulent confined coannular jets, *J. Fluid. Mech.*, 1996, 315, 387-412.
24. Ashurst, Wm. T. Constant density Markstein Flamelets in Navier Stokes turbulence, submitted to *Combust. Sci. and Tech.*
25. Candel, S. M. and Poinso, T. J. Flame Stretch and the balance equation for the flame area, 1990, *Combust. Sci. and Tech.*, 70, 1-15.

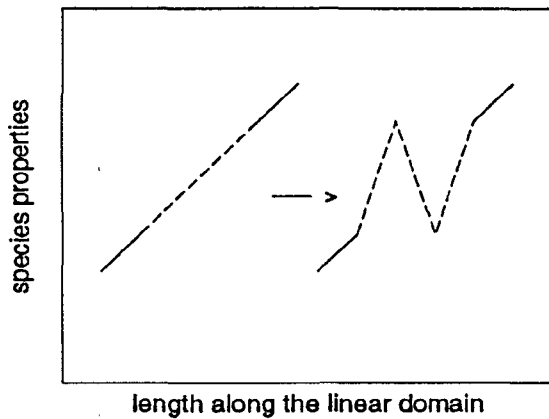


Figure 1: Illustration of triplet mapping

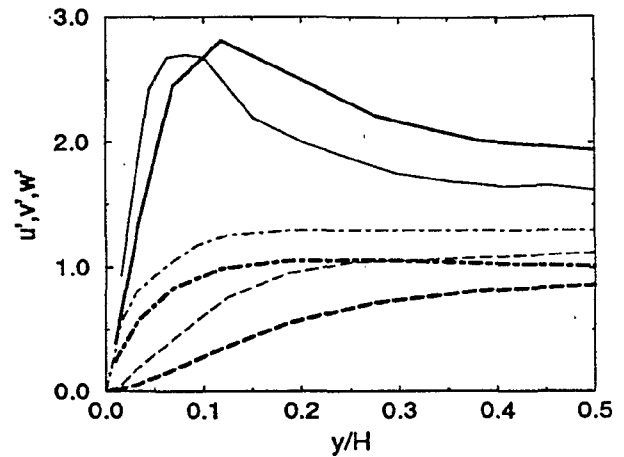


Figure 3: Rms velocities (non-dimensionalized by u^* , the friction velocity) in LES of Couette flow ($Re=5200$) on $25 \times 17 \times 17$ grid. Solid line: u_{rms} , dashed line: v_{rms} , dotted-dashed line: w_{rms} . Corresponding thinner lines indicate DNS data due to Bech et al.[22]

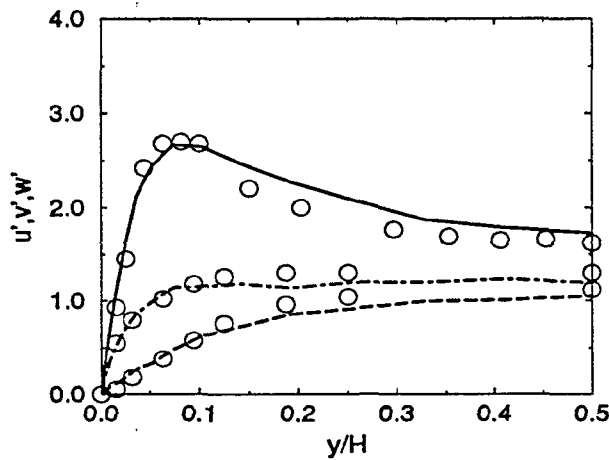


Figure 2: Rms velocities (non-dimensionalized by u^* , the friction velocity) in LES of Couette flow ($Re=5200$) on $49 \times 33 \times 33$ grid. Solid line: u_{rms} , dashed line: v_{rms} , dotted-dashed line: w_{rms} . Circles indicate DNS data due to Bech et al.[22].

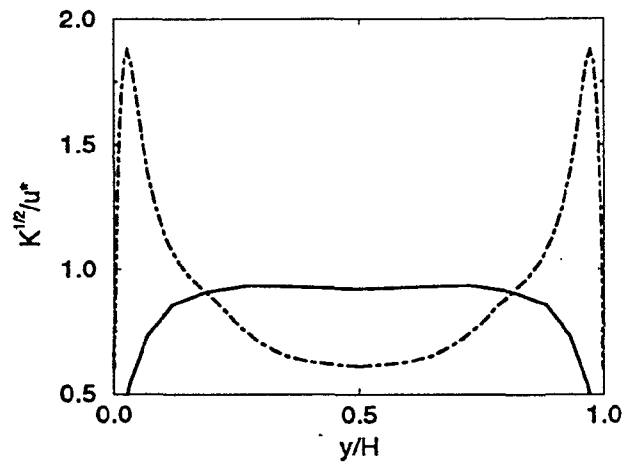


Figure 4: Subgrid kinetic energy in LES at $Re = 12,000$. Solid line: $25 \times 17 \times 17$ grid, dotted-dashed line: $65 \times 49 \times 49$ grid

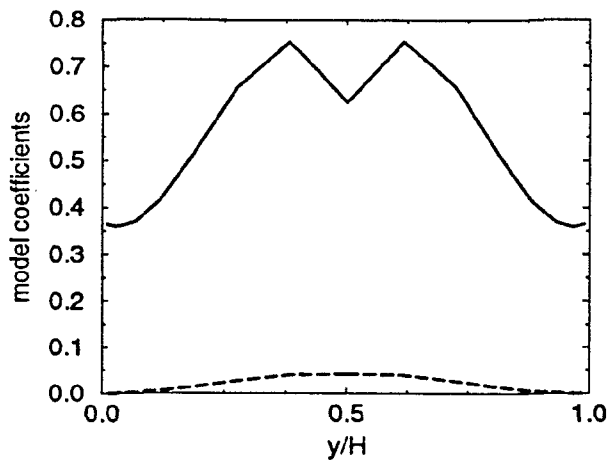


Figure 5: Variation of model coefficients computed using filtering approach. Solid line: C_e , dashed line: C_v

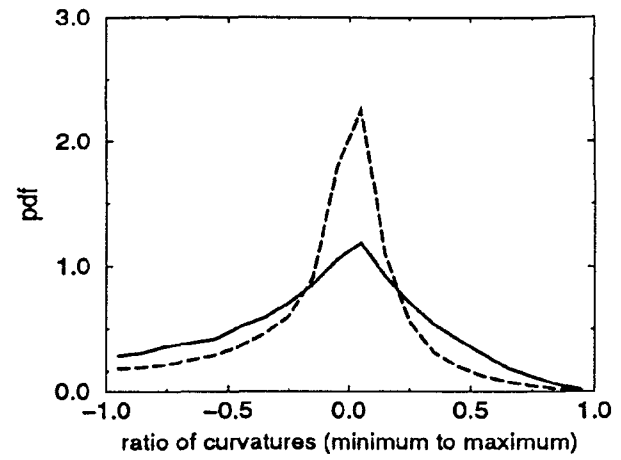


Figure 7: Pdf of the shape factor for $\frac{u'}{S_i} = 1$. Solid line: LEM, dashed line: Yakhot's model

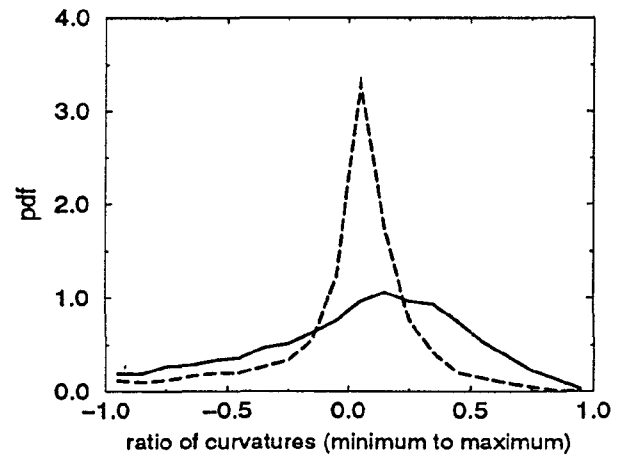


Figure 8: Pdf of the shape factor for $\frac{u'}{S_i} = 4$. Solid line: LEM, dashed line: Yakhot's model

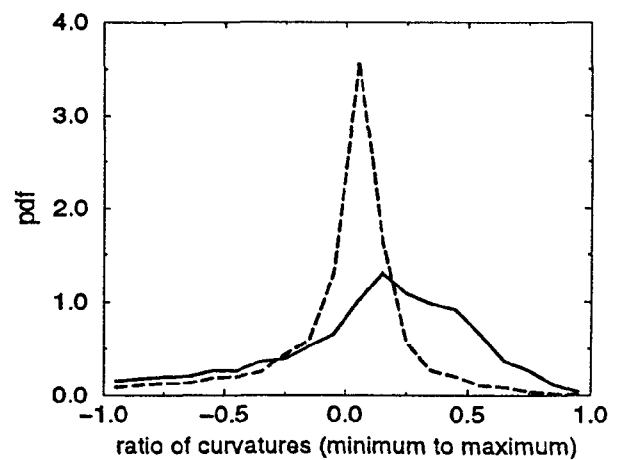


Figure 9: Pdf of the shape factor for $\frac{u'}{S_i} = 8$. Solid line: LEM, dashed line: Yakhot's model

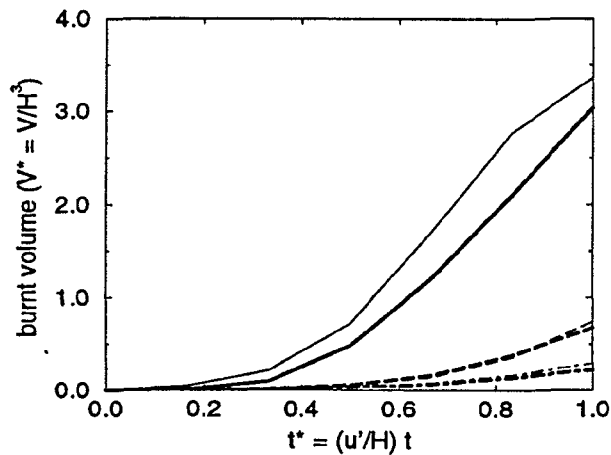


Figure 6: Temporal variation of volume occupied by burnt fluid in LES on a 65x49x49 grid. Solid line: $\frac{u'}{S_i} = 1$, dashed line: $\frac{u'}{S_i} = 4$, dotted-dashed line: $\frac{u'}{S_i} = 8$. The thinner lines indicate corresponding predictions from LES using Yakhot's model.

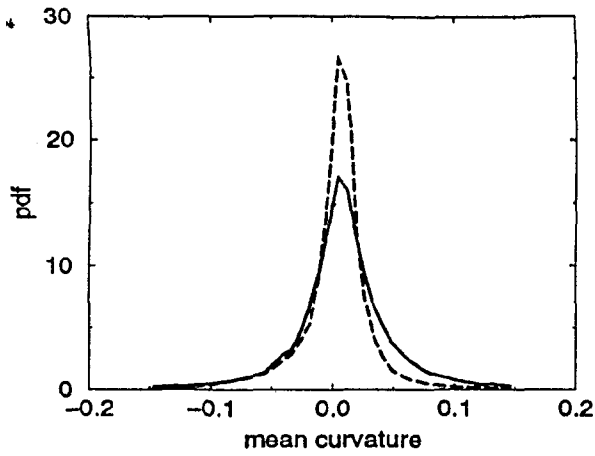


Figure 10: Pdf of the mean curvature for $\frac{u'}{S_1} = 1$. Solid line: LEM, dashed line: Yakhot's model

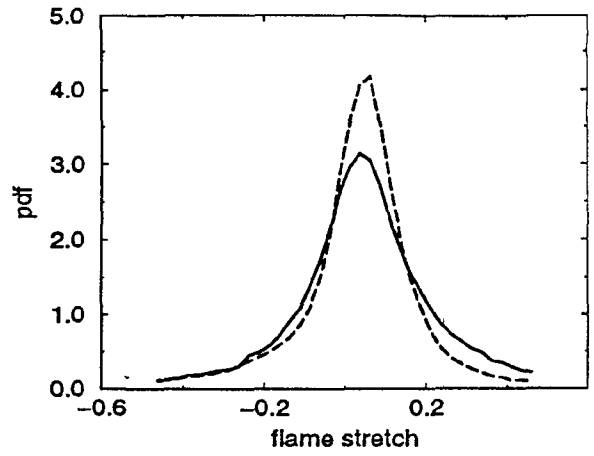


Figure 13: Pdf of the flame stretch for $\frac{u'}{S_1} = 1$. Solid line: LEM, dashed line: Yakhot's model

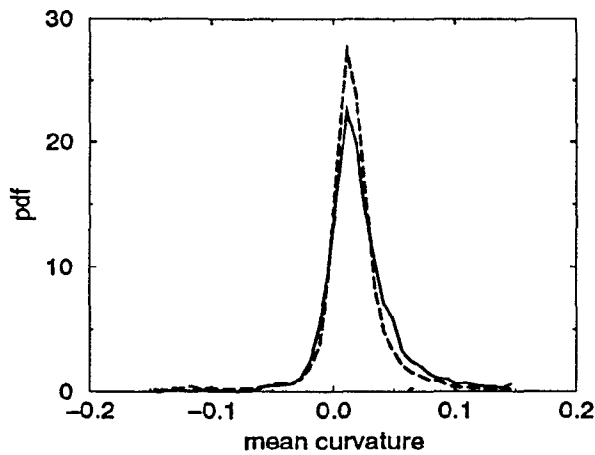


Figure 11: Pdf of the mean curvature for $\frac{u'}{S_1} = 4$. Solid line: LEM, dashed line: Yakhot's model

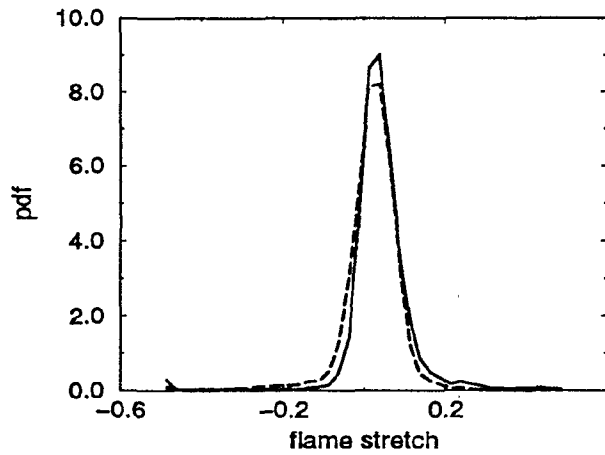


Figure 14: Pdf of the flame stretch for $\frac{u'}{S_1} = 4$. Solid line: LEM, dashed line: Yakhot's model

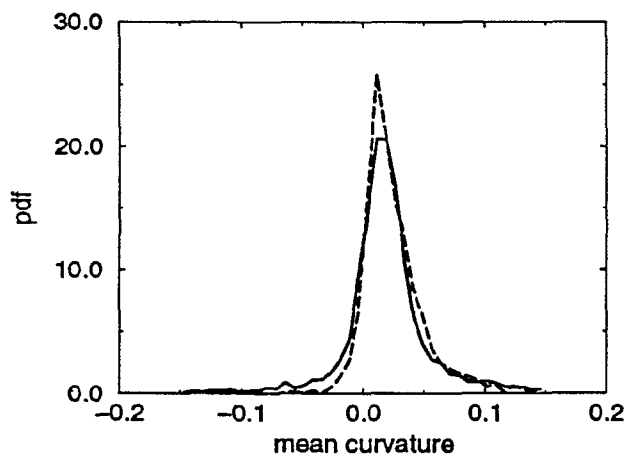


Figure 12: Pdf of the mean curvature for $\frac{u'}{S_1} = 8$. Solid line: LEM, dashed line: Yakhot's model

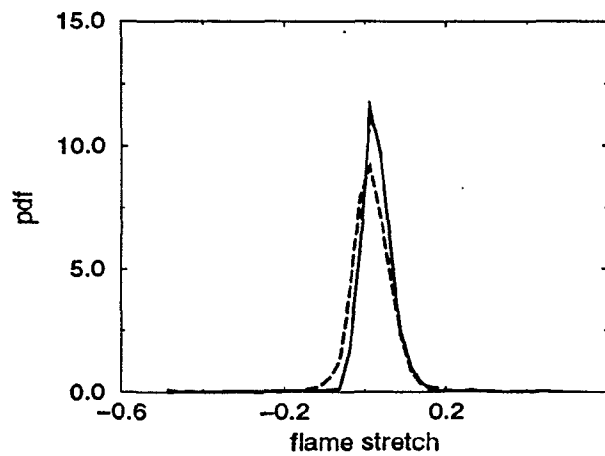


Figure 15: Pdf of the flame stretch for $\frac{u'}{S_1} = 8$. Solid line: LEM, dashed line: Yakhot's model

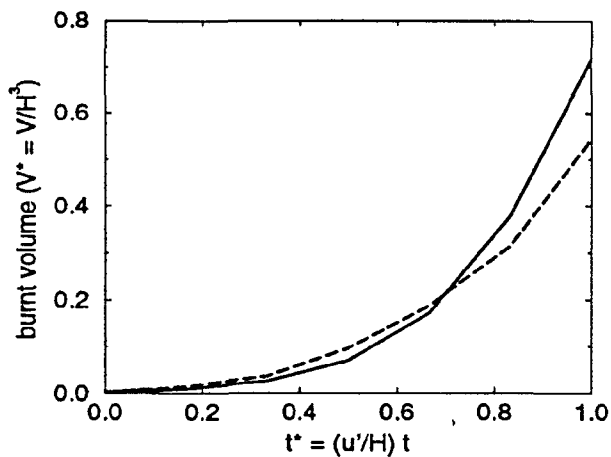


Figure 16: Temporal variation of volume occupied by burnt fluid in LES on a 25x17x17 grid. Solid line: LEM on a 25x17x17 grid, dashed line: Yakhot's model on a 65x49x49 grid.

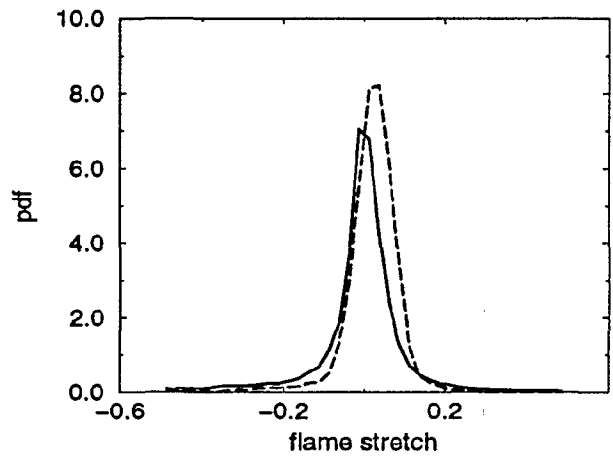


Figure 18: Pdf of flame stretch predicted by LES on 25X17X17 grid. Solid line: LEM, dashed line: LES using Yakhot's model on 65x49x49 grid.

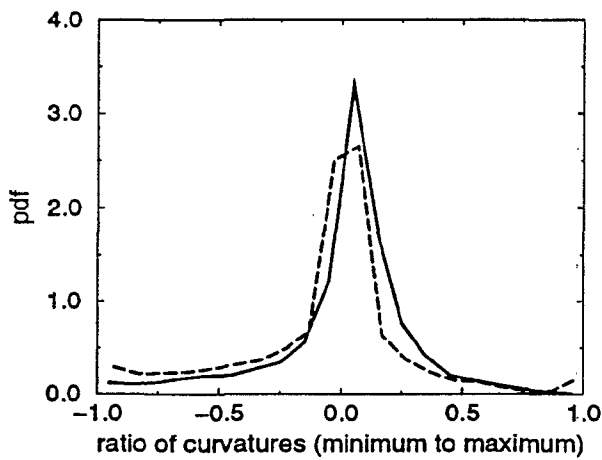


Figure 17: Shape factor of the flame predicted by LES on 25X17X17 grid. Solid line: LEM, dashed line: LES using Yakhot's model on 65x49x49 grid.